RSC Advances

PAPER

View Article Online
View Journal | View Issue

Cite this: *RSC Adv.*, 2026, **16**, 23078

Green-synthesized *Matricaria chamomilla* silver nanoparticles enhance anticonvulsant and neuroprotective effects through GABAergic and antioxidant pathways in an acute seizure rat model

Yahya Alhamhoom,[a] Rupesh Kumar M, *[b] Manjunath C,[b] Kavitha K,[c] Mohamed Rahamathulla,[a] Hanan Albataineh,[d] Syeda Ayesha Farhana,[e] Mohammed Muqtader Ahmed,[f] Thippeswamy Boreddy Shivanandappa[g] and Ismail Pasha *[h]

Epilepsy is a major chronic neurological disorder with significant treatment limitations, particularly in drug-resistant cases, highlighting the need for novel and affordable neuroprotective strategies. This study investigates the anticonvulsant and neuroprotective effects of ethanolic extract of *Matricaria chamomilla* (German chamomile) and its green-synthesized silver nanoparticles (MC-AgNPs) in a pentylenetetrazole (PTZ)-induced rat model. The phytochemical analysis (TPC, TFC, GC-MS) showed high phenolic (18.64 mg GAE per g) and flavonoid (17.04 mg QE per g) content with apigenin and quercetin identified as major constituents. Green-synthesized MC-AgNPs exhibit significant characteristics such as an SPR peak at 420 nm and a hydrodynamic diameter of 273.9 nm, indicating their stability and potential for neuroprotective applications. The administration of crude extract or MC-AgNPs (25 or 50 mg kg^{-1} p.o) for three days prior to PTZ induction results in substantial improvements. The high dose of MC-AgNPs notably increased seizure latency (69.33 ± 1.08 s), decreased seizure frequency (1.16 ± 0.16), and reduced seizure duration (9.5 ± 0.17 s), far exceeding the crude extract's effects ($p < 0.0001$). Furthermore, motor performance and memory retention were significantly enhanced, with GABA levels restored (5.1 ± 0.14 μmol g^{-1} tissue) and oxidative stress parameters improved. The histopathological assessments revealed minimal neuronal damage. Overall, MC-AgNPs demonstrated superior efficacy compared to the crude extract, indicating that nano-formulation could enhance the therapeutic potential of plant-derived agents in epilepsy management, suggesting a cost-effective adjunct therapy deserving further research studies.

Received 11th February 2026
Accepted 18th April 2026

DOI: 10.1039/d6ra01236a

rsc.li/rsc-advances

1. Introduction

Epilepsy is a chronic neurological condition characterized by frequent, unprovoked seizures brought on by aberrant central nervous system neuronal activity. It is still one of the most prevalent brain illnesses, affecting over 50 million individuals globally.[1–3] According to the ILAE, it is defined as an epileptic syndrome, a single seizure with a high chance of recurrence, or a series of unprovoked seizures spaced out by 24 hours. Its causes include structural, genetic, metabolic, infectious, or immune factors.[4,5] Symptoms range from convulsions and sensory disturbances to cognitive and psychiatric issues such as anxiety and depression.[6,7] Despite the availability of various antiepileptic medicines (AEDs), over one-third of people continue to have uncontrolled seizures, highlighting the critical need for safer, more economical, and more effective options for therapy.[8–10] Pentylenetetrazole (PTZ), a non-competitive GABA-A receptor antagonist, is commonly used to simulate generalized

[a]*Department of Pharmaceutics, College of Pharmacy, King Khalid University, Al Faraa, Abha 62223, Saudi Arabia. E-mail: ysalhamhoom@kku.edu.sa; rahapharm@gmail.com*

[b]*Department of Pharmacology, Al-Ameen College of Pharmacy, Bengaluru, Karnataka, India. E-mail: manirupeshkumar@yahoo.in; shekarmanju600@gmail.com*

[c]*Department of Pharmaceutics, Nitte College of Pharmaceutical Sciences, Nitte (Deemed to be University), Bengaluru, Karnataka, India. E-mail: kavitha.k@nitte.edu.in*

[d]*Pharmacy Department, College of Pharmacy, Amman Arab University, 11953 Amman, Jordan. E-mail: h.bataineh@aau.edu.jo*

[e]*Department of Pharmaceutics, College of Pharmacy, Qassim University, Buraidah 51452, Saudi Arabia. E-mail: a.farhana@qu.edu.sa*

[f]*Department of Pharmaceutics, College of Pharmacy, Prince Sattam Bin Abdul Aziz University, Al Kharj 11942, Saudi Arabia. E-mail: muqtadernano@gmail.com*

[g]*Department of Biomedical Science, College of Pharmacy, Shaqra University, Al-Dawadmi Campus, Dawadmi 11961, Saudi Arabia. E-mail: drswamy@su.edu.sa*

[h]*Department of Pharmacology, Orotta College of Medicine and Health Science, Asmara 10549, Eritrea. E-mail: ismail.orotta@gmail.com*

clonic seizures and important characteristics of human epilepsy, including GABAergic dysfunction, oxidative stress, cognitive impairment, and neuronal degeneration.[11–13]

Matricaria chamomilla L. is a common medicinal herb that belongs to the Asteraceae family and is prized for its versatility and variety of therapeutic uses.[14] Traditionally utilized across Europe, Asia, and the Middle East, it has been applied in treating digestive, respiratory, skin, pain, cancer and inflammatory disorders.[15–17] Its anti-inflammatory, antibacterial, and antioxidant properties are attributed to flavonoids as well as essential oils high in α-bisabolol and chamazulene found in its blossoms. Ethnopharmacological records show its use in teas, extracts, and oils for both internal and topical treatments. Its strong safety record, cultural acceptance, and wide pharmacological potential make it a valued plant in both traditional and modern medicine. *M. chamomilla* has a variety of pharmacological effects beyond its conventional uses, such as antioxidant, anti-inflammatory, antimicrobial, anxiolytic, wound-healing, and neuroprotective properties.[18–20] The flavonoid apigenin is especially notable for its positive allosteric modulation of GABA-A receptors, producing sedative, anxiolytic, and anticonvulsant effects in preclinical models.[21] Studies show that chamomile extracts help reduce oxidative stress, regulate neurotransmission, and protect neurons from seizure-induced damage.[22] These properties highlight its potential as an adjunct or alternative therapy for epilepsy, offering neuroprotective advantages often lacking in conventional antiepileptic drugs.[23] Through mechanisms involving GABAergic modulation and antioxidant pathways, chamomile's phytoconstituents provide scientific support for its traditional use in seizure management.

The therapeutic efficacy of phytochemicals in neurological disorders is constrained by inadequate bioavailability and limited permeability across the blood–brain barrier (BBB). Delivery systems based on nanotechnology, especially green-synthesized silver nanoparticles (AgNPs), provide a biocompatible approach to address these challenges.[24,25] AgNPs improve the stability, solubility, cellular uptake, and blood–brain barrier penetration of bioactive phytoconstituents, while also demonstrating inherent antioxidant and anti-inflammatory effects in neurological models.[26–28] So far, no studies have been conducted to evaluate the anticonvulsant effectiveness of *Matricaria chamomilla*-induced silver nanoparticles (MC AgNPs) in experimental epilepsy.

This work is novel since it is the first to show the neuroprotective and antiepileptic effects of green synthesized silver nanoparticles derived from *Matricaria chamomilla* (MC AgNPs) in a pentylenetetrazole (PTZ) induced acute seizure rat model. Previous reports only focused on the crude extract. This study includes a full mechanistic evaluation that includes phytochemical characterization, nanoparticle profiling, behavioral assays, neurochemical quantification, oxidative stress biomarkers, and quantitative hippocampal histopathology—to compare the efficacy of the nanoformulation against the crude extract. We hypothesis that green-synthesized MC-AgNPs will exhibit greater anticonvulsant and neuroprotective efficacy than crude extract, facilitated by improved bioavailability and synergistic modulation of GABAergic and antioxidant pathways.

2. Methodology

2.1. Collection and authentication of plant material

The flowers of *Matricaria chamomilla* were procured from Ikon Aromatics and Herbs Pvt. Ltd. The Central Ayurveda Research Institute, Uttarahalli, Bengaluru, identified and verified the plant material (Authentication no./SMPU/CARI/BNG/2025-26/1590). The authenticated plant material was cleaned, shade-dried, and finely powdered for extraction.

2.2. Preparation of ethanolic extract

Chamomile flowers (50 g) were extracted with 70% ethanol (250 mL) using a magnetic stirrer and kept overnight. To acquire the alcoholic extract, the mixture was filtered, and a rotary evaporator was used to concentrate the filtrate at 40 °C at lower pressure. The dried extract in a sealed container was stored at 4 °C for later use.[29] Its antioxidant, anti-inflammatory, neuroprotective, and anticonvulsant qualities are attributed to flavonoids (apigenin, luteolin, and quercetin), terpenoids, tannins, glycosides, alkaloids, and phenolic substances, all of which were verified by phytochemical screening.

2.3. Phytochemical characterization

2.3.1. Determination of total phenolic content (TPC). The TPC was determined using the spectrophotometric method. The total phenolic content was determined using the Folin–Ciocalteu method. 1 mL of the extract sample (1 mg mL^{-1}) was mixed with Folin–Ciocalteu's reagent and sodium carbonate, along with distilled water. Absorbance at 750 nm was obtained following a 90-minute dark incubation period at 23 °C. TPC was calculated using a gallic acid calibration curve, and results were expressed as milligrams of gallic acid equivalents (GAE) per gram of dry material.[30,31]

2.3.2. Determination of total flavonoid content (TFC). The aluminium chloride ($AlCl_3$) colorimetric method was used for the determination of *M. chamomilla*'s TFC, with quercetin serving as a standard. The extract solution was treated with $NaNO_2$, $AlCl_0$, and NaOH one at a time.[32] Then, methanol was added to thin the mixture out, and it was left to turn color. A quercetin calibration curve was used to calculate TFC, which was then expressed as μg quercetin equivalents (QE) per mg of dry weight. Absorbance was measured at 510 nm.[33]

2.3.3. Gas chromatography-mass spectrometry (GC-MS) analysis. A GC-MS analysis of *M. chamomilla* was conducted using a Clarus 680 GC fitted with an Elite-5MS column (30 m × 0.25 mm × 250 μm) and helium as a carrier gas (1 mL min^{-1}). The injector was set to 260 °C, the oven was set to 60–300 °C at 10°C min^{-1} (hold 6 min), and the injection volume was 1 μL. Compounds were recognized using the NIST (2008) library, and mass spectra were acquired using electron impact ionization (70 eV), with a scan range of 40–600 Da.[34]

2.4. Green synthesis of silver nanoparticles of *Matricaria chamomilla*

To perform the green synthesis, combine 90 mL of 0.1 M $AgNO_3$ solution with 10 mL of *M. chamomilla* ethanolic extract, and stir

for 30 minutes at 60 °C. The silver nanoparticles that were developed were visually confirmed by a color change to brown, confirming the formation of nanoparticles. The mixture was centrifuged at 15 000 rpm for 30 minutes at 4 °C and stored in an amber vial at 4 °C for further analysis. The resulting pellets were rinsed with distilled water, dried at 60 °C, and kept for further analysis. For *in vivo* administration, the nanoparticle material was freshly dispersed in sterile saline *via* brief ultrasonication for 5 minutes (40 kHz) to achieve a uniform suspension.[35]

Optimal synthesis conditions were determined during preliminary trials. The optimal volume ratio of extract to 0.1 M $AgNO_3$ was 1 : 9 (v/v), resulting in the most intense and stable surface plasmon resonance (SPR) peak. The pH of the reaction mixture was adjusted to 6.5 with 0.1 M NaOH or HCl, which promoted maximum bioreduction and little aggregation. Lower temperatures (25–40 °C) caused slower nanoparticle generation, while higher temperatures (≥80 °C) caused aggregation. Therefore, the reaction temperature was kept at 60 °C. These modified settings consistently produced MC AgNPs with predictable SPR and colloidal properties.

2.5. Characterization of silver nanoparticles of *Matricaria chamomilla* (MC-AgNPs)

2.5.1. UV-visible spectroscopy. The formation of MC-AgNPs was initially confirmed by their surface plasmon resonance (SPR) spectrum in the range of the 200–800 nm region using UV-visible spectroscopy (Shimadzu UV-1900i).

2.5.2. Dynamic light scattering (DLS) and zeta potential. In order to determine the surface charge, hydrodynamic diameter, and size distribution (polydispersity index, PDI) of MC-AgNPs, a Malvern Zetasizer ZS (Malvern Instruments, UK) was utilized. Prior to analysis, the nanoparticles were uniformly dispersed in deionized water at a concentration of 1 mg mL^{-1} and subjected to sonication for duration of one minute.[36] The experiments were performed in triplicate at 25 °C.

2.5.3. Fourier transform infrared spectroscopy (FTIR). Fourier transform infrared spectroscopy (FTIR) was used to identify functional groups involved in the reduction and stabilization of AgNPs, with spectra obtained between 400 and 4000 cm^{-1}.[37]

2.5.4. Scanning electron microscopy (SEM). A field-emission scanning electron microscope (Zeiss Gemini 500, Germany) was utilized in order to investigate the surface morphology of MC-AgNPs. A drop of nanoparticle suspension was placed on a silicon wafer, air-dried, and sputter-coated with a thin layer of gold before imaging at an accelerating voltage of 10 kV.[37]

2.6. Experimental animals

The adult healthy Wistar albino rats weighing 170–220 g were procured from the Central Animal House. The animals were kept in polypropylene cages containing sterile husk bedding under typical laboratory conditions, which included a 12-hour light/dark cycle, 25 ± 5 °C, and 40–60% humidity, with free access to food and water. Animals were acclimatized for one week before the experiment.[38] All operations adhered to CPCSEA norms and were authorized by the Institutional Animal Ethics Committee (approval no: AACP/IAEC/41/MARCH 2025/09) of Al-Ameen College of Pharmacy, Bengaluru. India.

2.7. Experimental design

In the experimental design seven groups ($n = 6$), a total of 42 albino rats, were used. Three days of oral treatment with either vehicle (control), diazepam (5 mg kg^{-1}, standard), or *M. chamomilla* extract or MC-AgNPs at low and high dosages were administered to six rats per group. PTZ was given an hour after the last dose, and seizure activity was tracked for 30 minutes. Survival and delayed effects were noted for up to 24 hours. Mortality, seizure length and intensity, latency to clonic seizures, and time to tonic convulsions were among the parameters assessed.[39,40] This design allowed comparison between untreated controls, PTZ-induced negative controls, a standard anticonvulsant group, and test groups receiving low and high doses of *M. chamomilla* ethanolic extract and silver nanoparticles. It provided a clear framework to assess dose-dependent effects and compare the efficacy of the test formulations with the standard drug (Table 1). The *in vivo* experiments were conducted from July 10, 2025 to July 24, 2025.

2.8. Induction of epilepsy

The epileptic seizures in Wistar rats were induced by PTZ (80 mg kg^{-1}, i.p.), which inhibits GABA-A receptors to cause epilepsy. The rats received treatments once daily for three days before PTZ administration.[41,42]

2.9. Behavioral assessment of seizures

After PTZ administration, rats were monitored individually for 30 min for acute seizures and 24 h for delayed effects and

Table 1 Experimental design of all groups (I–VII)

Group	Treatment	Drug/dose	Route of administration
Group-I	Normal control	Vehicle (saline, 10 mL kg^{-1})	Oral (p.o.)
Group-II	Negative control	PTZ-induced control (80 mg kg^{-1})	Intraperitoneal (i.p.)
Group-III	Standard	Diazepam (5 mg kg^{-1}) + PTZ (80 mg kg^{-1})	Diazepam – p.o., PTZ – i.p.
Group-IV	Test (low dose)	*M. chamomilla* ethanolic extract (55 mg kg^{-1}) + PTZ (80 mg kg^{-1})	Extract – p.o., PTZ – i.p.
Group-V	Test (high dose)	*M. chamomilla* ethanolic extract (110 mg kg^{-1}) + PTZ (80 mg kg^{-1})	Extract – p.o., PTZ – i.p.
Group-VI	Test (low dose)	MC-AgNPs (25 mg kg^{-1}) + PTZ (80 mg kg^{-1})	Extract – p.o., PTZ – i.p.
Group-VII	Test (high dose)	MC-AgNPs (50 mg kg^{-1}) + PTZ (80 mg kg^{-1})	Extract – p.o., PTZ – i.p.

mortality. Parameters recorded included latency to clonic and tonic seizures, total seizure duration, severity and 24-hour survival (modified Racine's scale, stages 1–5)[43,44] The protective effects of diazepam, *M. chamomilla* extract, and its silver nanoparticles may therefore be compared both quantitatively and qualitatively. To reduce variability, all behavioral tests were conducted by a single observer who was blinded to the treatment groups, and the animals were carefully matched for body weight, age, and timing of PTZ administration.

2.10. Assessment of cognitive and muscle coordination

The effects of the formulations on cognitive function and neuromuscular coordination were evaluated using the passive avoidance test and the Rotarod. These models are widely used to study seizure-induced neurocognitive deficits and the protective efficacy of therapeutic agents.[44–46]

2.10.1. Passive avoidance test. The neuroprotective effect of *M. chamomilla* extract has been assessed using the passive avoidance test. Rats were given a minor foot shock and trained to avoid a dark chamber. Step-through latency and time in the dark compartment (TDC) were measured after a 24-hour period. Increased STL and reduced TDC indicated improved memory retention, demonstrating the extract's protective effect against PTZ-induced cognitive deficits.

2.10.2. Rotarod test. Motor coordination and neuromuscular performance were evaluated using the Rotarod test.[46] Rats were trained to stay on a 7 cm rotating rod at 20 rpm for 180 s. Twenty-four hours after PTZ, fall-off latency was measured over three trials per rat (15 min intervals), and the mean latency was calculated, with a 180 s cut-off.

2.11. Estimation of γ-aminobutyric acid (GABA) in rat brain

The colorimetric test of phenol–hypochlorite was used to determine the amount of GABA in the brain. After the trial was over, around 100 mg of brain tissue was mixed with 1 mL of 0.1 M phosphate buffer (pH 7.4) and was centrifuged for 10 minutes at 4 °C at 12 000 rpm. The supernatant (0.4 mL) was reacted with sodium carbonate, sodium borate buffer, phenol, and sodium hypochlorite, incubated, boiled, cooled, and stabilized with 60% ethanol. Absorbance at 640 nm was compared to a GABA standard curve, and levels were expressed as μ mol g^{-1} wet tissue.[47]

2.12. Assessment of oxidative stress markers

Superoxide dismutase (SOD) for enzymatic antioxidant defence, reduced glutathione (GSH) for non-enzymatic antioxidant capacity, and malondialdehyde (MDA) for lipid peroxidation were the three main oxidative stress indicators that were assessed in brain tissue to assess seizure-induced neuronal damage. Rats were sacrificed, their brains removed, cleaned with ice-cold saline, and blotted dry following behavioral evaluations. After blending the tissues in 10% w/v ice-cold 0.1 M phosphate-buffered saline, they were centrifuged for 15 minutes at 10 000 rpm and 4 °C. After being collected, the supernatant was utilized for biochemical tests.[48,49]

2.13. Histopathological studies

Brains were collected, preserved in 10% formalin, paraffin-embedded, and sectioned (5 μm) for H&E staining. Microscopic examination of the hippocampus and cortex assessed neuronal integrity, degeneration, cell density, gliosis, and vascular changes to evaluate the neuroprotective effects of *M. chamomilla* extract and MC-AgNPs against PTZ-induced damage.[50]

2.14. Euthanasia and tissue collection

After completing behavioral tests, rats were decapitated under deep anaesthesia induced by an intraperitoneal dose of ketamine (80 mg kg^{-1}) and xylazine (10 mg kg^{-1}). This technique was executed in strict conformity with the American Veterinary Medical Association (AVMA) Guidelines for the Euthanasia of Animals. Brain tissues were immediately removed, washed in ice-cold saline, and processed for biochemical and histological investigations.

2.15. Statistical analysis

All results are presented as mean ± SEM ($n = 6$). Statistical analysis was carried out using GraphPad Prism (version 9.0). To determine differences between groups, a one-way analysis of variance (ANOVA) was performed, followed by Tukey's post hoc test for multiple comparisons. A p-value of less than 0.05 was considered statistically significant. Tukey's test was used specifically to compare the test groups with both the negative control (PTZ-induced) group and the standard (diazepam) group.[51]

3. Results

3.1. Total phenolic content (TPC)

The ethanol extract of *M. chamomilla* had a total phenolic content of 18.64 mg GAE per g, measured using the gallic acid calibration curve ($R^2 = 0.9925$). The significant phenolic content supports its putative antioxidant and neuroprotective effects (Fig. S1).

3.2. Total flavonoid content (TFC)

The extract had a TFC of 17.04 mg QE per g, estimated with a quercetin calibration curve ($R^2 = 0.9856$). The presence of flavonoids, notably apigenin and quercetin, implies potential GABAergic regulation (Fig. S2).

3.3. GC-MS analysis

One gram of *M. chamomilla* ethanolic extract was analyzed by GC-MS at Vellore Institute of Technology, revealing a variety of compounds with distinct retention times and molecular weights. Notably, the flavonoids apigenin and quercetin were identified based on their mass spectra and retention times: apigenin at RT 18.23 min (molecular weight 270.24, match factor 92%) and quercetin at RT 20.06 min (molecular weight 302.24, match factor 94%). These flavonoids are well-known for their GABAergic and antioxidant properties and are thought to

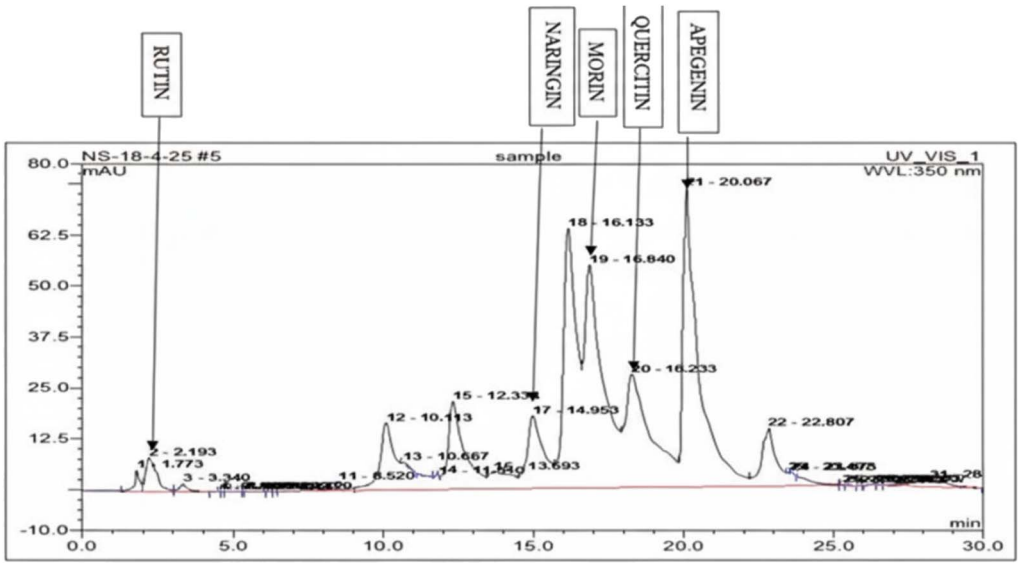

Fig. 1 GCMS graph of *Matricaria chamomilla* Ethanolic extract.

play key roles in both the bioreduction and capping of silver nanoparticles. The chromatogram is shown in Fig. 1.

3.4. Characterization of MC silver nano particles

Characterization of silver nanoparticles determines their size, shape, surface charge, and stability, which influence their biological and physicochemical properties. It confirms successful synthesis, ensures reproducibility, and helps correlate nanoparticle features with therapeutic or functional activities.[52]

3.4.1. UV-visible spectroscopy. The UV-vis spectrum of silver nanoparticles synthesized using *M. chamomilla* extract was recorded in the 200–800 nm range. At 400–450 nm, a distinctive surface plasmon resonance (SPR) peak was seen, and the wide peak indicated the polydispersity of the nanoparticles. The MC-AgNPs exhibited a distinct surface plasmon resonance (SPR) peak at 420 nm, confirming successful nanoparticle formation (Fig. S3).

3.4.2. Particle size and PDI analysis. According to DLS analysis showed that the nanoparticles had an average hydrodynamic diameter of 273.9 ± 4.4 nm, with a polydispersity index (PDI) of 0.312. This size reflects not just the metal core but also the surrounding phytochemical coating (known as the biomolecular corona) and some minor particle clustering. While the individual silver cores are typically much smaller—around 20 to 100 nm—the larger measured size is consistent with biologically synthesized nanoparticles that are stabilized by a thick

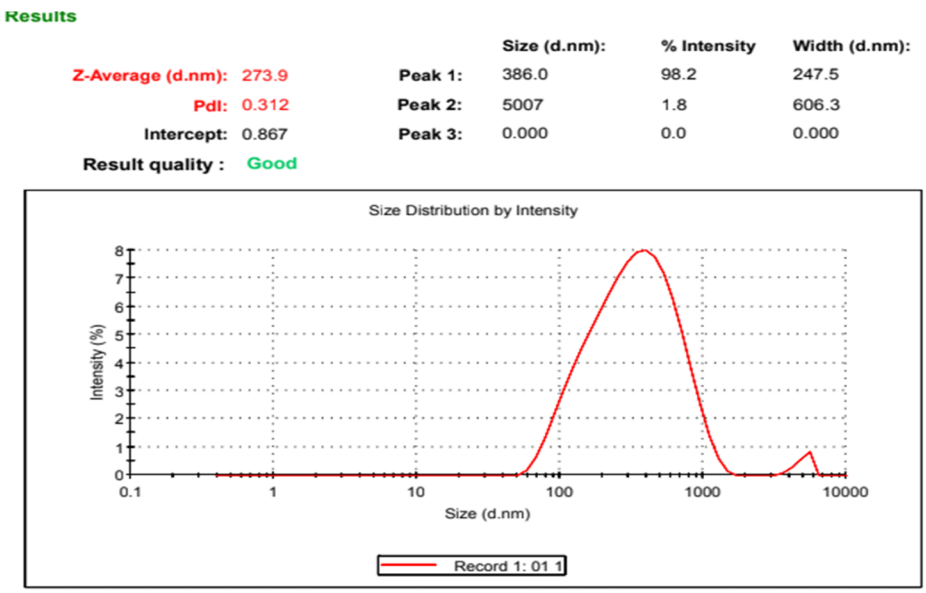

Fig. 2 Particle size analysis of MC AgNPs.

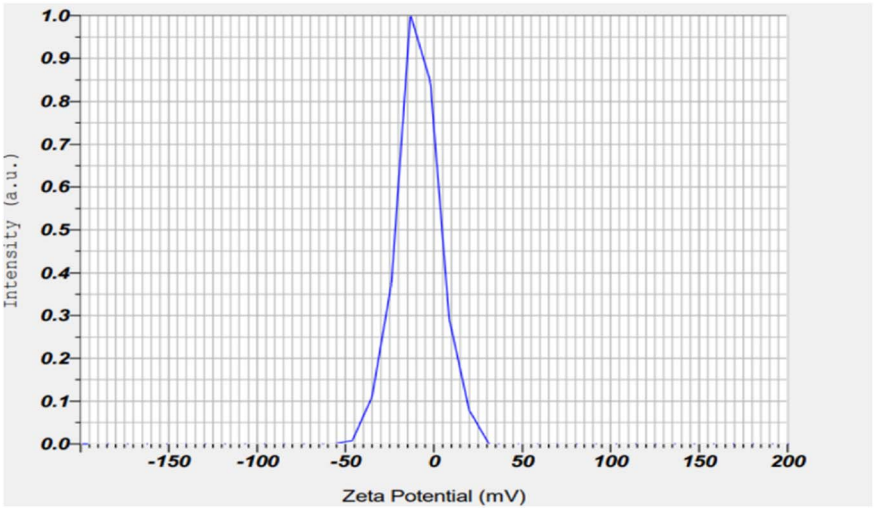

Fig. 3 Zeta potential silver nanoparticles.

organic layer. The PDI value of 0.312 indicates moderate variation in particle size, which is considered acceptable for green-synthesized nanoparticles and suggests a fairly uniform size distribution (Fig. 2).

3.4.3. Zeta potential. The zeta potential of the MC AgNPs was measured at -8.9 ± 0.08 mV. This value falls within the range that indicates limited electrostatic stabilization (between 0 and ± 10 mV), meaning the nanoparticles don't have enough surface charge to keep them from clumping together through electrostatic repulsion alone. Instead, their stability is likely maintained mainly by a steric barrier formed by the phytochemical coating—such as flavonoids and phenolics—on the nanoparticle surface. This natural coating helps prevent the particles from aggregating and could also affect how the nanoparticles behave inside the body (Fig. 3).

3.4.4. Fourier-transform infrared spectroscopy. The ATR FTIR analysis was used to identify the key functional groups involved in reducing and stabilizing the MC AgNPs (see Fig. 4). The FTIR spectrum showed distinctive peaks at 3269 cm^{-1}, corresponding to O–H stretching from phenols and alcohols; 2919 cm^{-1}, related to C–H stretching in aromatic compounds; 1629 cm^{-1}, indicating C=O stretching typical of flavonoids; and a broad band between 1367 and 1013 cm^{-1}, representing C–O stretching vibrations. These findings confirm the presence of phenolic and flavonoid compounds, which play important roles as both reducing and capping agents during the green synthesis of silver nanoparticles. Similar functional groups have been reported in previous studies on Matricaria chamomilla-mediated silver nanoparticles (Dadashpour *et al.*, 2018; Alsheri *et al.*, 2020), supporting the idea that these plant compounds are crucial for converting silver ions into stable, biocompatible nanoparticles while preventing them from clumping together.

3.4.5. Scanning electron microscopy (SEM). The SEM analysis revealed that the synthesized silver nanoparticles were mostly spherical, featuring smooth surfaces and clear, well-defined edges.

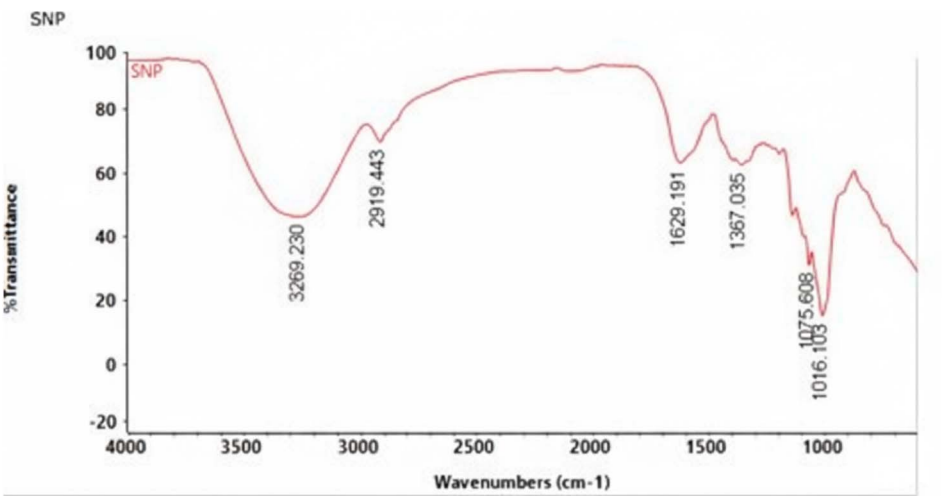

Fig. 4 IR spectra for biosynthesised silver nanoparticles of *Matricaria chamomilla*.

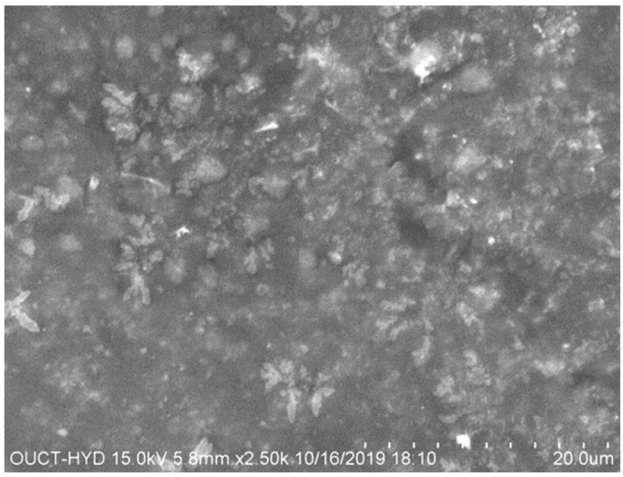

Fig. 5 SEM Analysis of HEMC AgNPs.

The particles were evenly spread out, with only minor clumping, which is likely caused by the phytochemical coating or the drying process during sample preparation. These results confirm successful formation of nanoparticles with a suitable shape and stability for potential pharmacological applications (Fig. 5). Although EDX and XRD analyses were not conducted in this study due to limited access to the equipment, we recommend including these techniques in future research to verify the elemental composition and crystal structure of the nanoparticles.

3.5. Effect of treatments on seizure onset and protection

The PTZ administration rapidly induced tonic–clonic seizures in group II, confirming its pro-convulsant activity. Diazepam (4 mg kg^{-1}) provided complete protection and significantly prolonged seizure onset (73 ± 1.23 s $p < 0.0001$). The *M. chamomilla* extract (HEMC) produced dose-dependent anticonvulsant effects (45 ± 1.52 s $p < 0.0001$.), whereas the silver nanoparticle formulation (MC-AgNPs) produced markedly superior protection (69.33 ± 1.08 s, $p < 0.0001$). High-dose MC-AgNPs (50 mg kg^{-1}) nearly matched diazepam in delaying seizure onset and protecting all animals against seizures and mortality (Fig. 6; Table 2).

Statistical analysis showed highly significant differences ($p < 0.05$ to $p < 0.0001$). The low SEM values reflect the remarkable consistency within groups attained by strictly standardising experimental conditions. Complete protection was defined as 100% survival and the absence of tonic-clonic seizures, in accordance with standard PTZ model protocols.

Each value is presented as mean ± SEM, with six animals per group. Dunnett's multiple comparison test was used to assess statistical significance after the data underwent a one-way ANOVA. The induced group and all treated groups were compared. * indicates $P < 0.05$, ** indicates $P < 0.01$, *** indicates $P < 0.0001$, and ns shows non-significant differences. A significance level of $P < 0.05$ was deemed statistically significant.

3.6. Effect of treatments on seizure frequency, severity, and duration

PTZ-treated rats recorded the highest seizure frequency, maximal severity (score 5), and prolonged duration. Diazepam significantly reduced seizure intensity and frequency. The MC-AgNPs demonstrated superior anticonvulsant activity: The high-dose MC AgNPs group exhibited the shortest seizure duration (9.50 ± 0.60 s), which was significantly lower than that of the PTZ group (28.60 ± 1.20 s, $p < 0.001$). Although the duration was also shorter than in the diazepam group (12.30 ± 0.90 s), this difference was not statistically significant ($p > 0.05$) (Fig. 7; Table 3).

The Tukey's post hoc analysis revealed that high dose MC AgNPs (50 mg kg^{-1}) significantly reduced seizure frequency, severity, and duration compared to the PTZ induced group ($p < 0.001$), and were not significantly different from the diazepam group for seizure frequency significant ($p < 0.05$ to $p < 0.01$) (Table 3).

3.7. Effect of treatments on cognitive function (passive avoidance test)

As expected, although diazepam effectively suppressed seizures, it impaired memory retention, leading to a shorter latency to enter the dark chamber and more time spent there—consistent

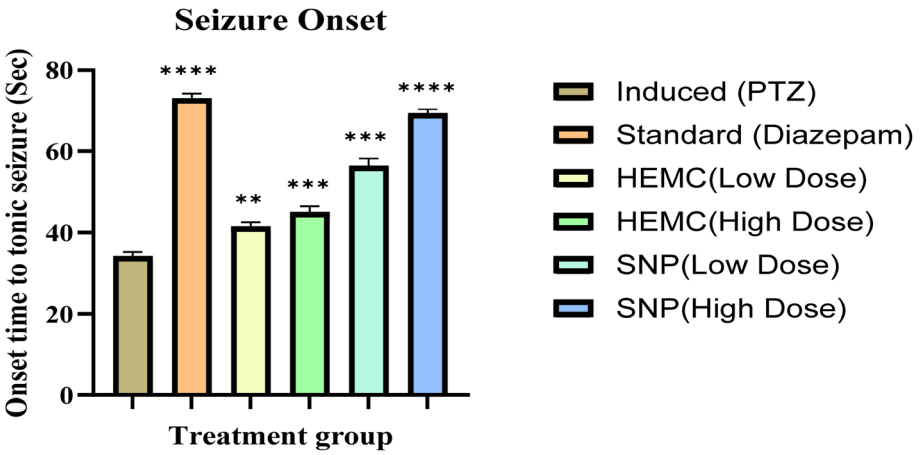

Fig. 6 Effect of treatment compounds of *Matricaria chamomilla* on seizure onset and protection of rats.

Table 2 Effect of treatments on seizure onset and protection

Group	Treatment	Onset time to tonic seizure (sec, mean ± SEM, $n = 6$)	Animals protected from tonic seizure (n/6)	Animals protected from death (n/6)
Group-I	Normal control (vehicle)	00	0	0
Group-II	Positive control	34.16 ± 1.04***	0	0
Group-III	Standard (diazepam, 5 mg kg^{-1})	73 ± 1.23****	6	6
Group-IV	HEMC (55 mg kg^{-1})	41.5 ± 1.08**	2	2
Group-V	HEMC (110 mg kg^{-1})	45 ± 1.52***	3	3
Group-VI	MC-AgNPs (25 mg kg^{-1})	56.3 ± 2.27***	4	4
Group-VII	MC-AgNPs (50 mg kg^{-1})	69.33 ± 1.08***	5	5

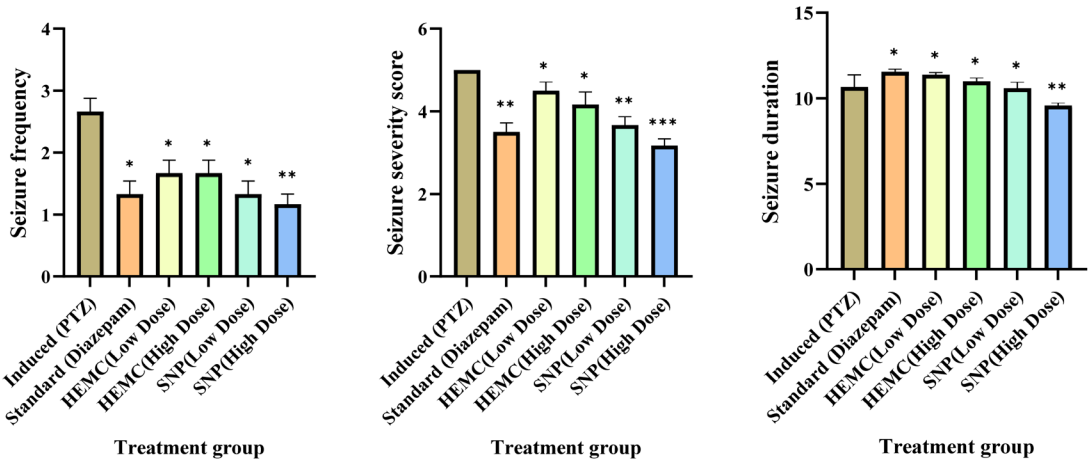

Fig. 7 Effect of treatment compounds of *Matricaria chamomilla* on seizure frequency, severity, and duration of rats.

Table 3 Effect of treatments on seizure frequency, severity, and duration[a]

Group	Treatment	Seizure frequency (per animal, mean ± SEM)	Seizure severity score (0–5 scale, mean ± SEM)	Seizure duration (sec, mean ± SEM)
Group-I	Normal control (vehicle)	0.00 ± 0.00	0.00 ± 0.00	0.00 ± 0.00
Group-II	PTZ-induced (80 mg kg^{-1})	2.66 ± 0.21	5.00 ± 0.00	28.60 ± 1.20
Group-III	Diazepam (5 mg kg^{-1}) + PTZ	1.33 ± 0.21***	3.50 ± 0.22***	12.30 ± 0.90 ***
Group-IV	HEMC (55 mg kg^{-1}) + PTZ	1.66 ± 0.21**	4.50 ± 0.22*	25.40 ± 0.80 *
Group-V	HEMC (110 mg kg^{-1}) + PTZ	1.33 ± 0.21*	1.66 ± 0.21**	22.50 ± 0.90 **
Group-VI	MC-AgNPs (25 mg kg^{-1}) + PTZ	1.33 ± 0.21 ***	3.66 ± 0.21***	3.66 ± 0.21 ***
Group-VII	MC-AgNPs (50 mg kg^{-1}) + PTZ	1.16 ± 0.16 ***	3.16 ± 0.16 ***	9.50 ± 0.60 ***

[a] All data are mean ± SEM ($n = 6$). *$p < 0.05$, **$p < 0.01$, ***$p < 0.001$ *vs.* PTZ-induced group. One-way ANOVA followed by Tukey's post-hoc test.

with its well-known amnestic effects. Treatment with HEMC improved cognitive outcomes in a dose-dependent manner. Notably, MC-AgNPs produced the strongest effect, with high-dose rats exhibiting the highest retention latency and longest duration in the light chamber, indicating substantial mitigation of PTZ-induced cognitive deficits. MC-AgNPs improved cognitive outcomes:—high-dose MC-AgNPs increased STL to 93.5 ± 0.99 s ($p < 0.0001$)—increased time spent in the light chamber (210.6 ± 0.88 s) showed in (Fig. 8; Table 4). The low SEM values indicate that cognitive performance was consistent within each group, likely due to the standardized experimental conditions and the use of a single blinded observer.

Each value presented as mean ± SEM, with six animals per group. Dunnett's multiple comparison test was used to assess statistical significance after the data underwent a one-way ANOVA. The induced group and all treated groups were compared. * indicates $P < 0.05$, ** indicates $P < 0.01$, *** indicates $P < 0.0001$, and ns shows non-significant differences. A significance level of $P < 0.05$ was deemed statistically significant.

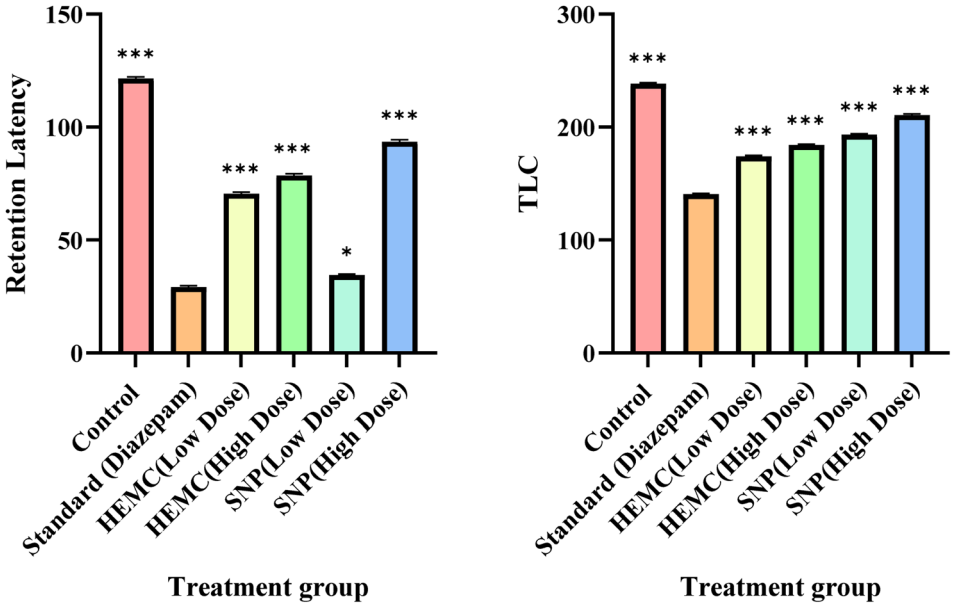

Fig. 8 Effect of treatment compounds of *Matricaria chamomilla* on cognitive function (passive avoidance test) of rats.

Table 4 Effect of treatments on cognitive function (passive avoidance test)

Group	Treatment	Acquisition trial latency to enter dark chamber (sec), mean ± SEMs	No. of shocks (N)	Retention trial latency to enter dark chamber (sec), mean ± SEM	Time spent in light chamber (sec), mean ± SEM
Group-I	Normal control	34.1 ± 0.60	1.83 ± 0.86	121.5 ± 0.76***	238.5 ± 0.76***
Group-II	Standard (diazepam, 4 mg kg^{-1})	34 ± 0.57	1.66 ± 0.71	29.166 ± 0.60	140.8 ± 0.60
Group-III	HEMC (55 mg kg^{-1})	34.5 ± 0.42	1.33 ± 0.71	70.5 ± 0.76***	174.1 ± 0.60***
Group-IV	HEMC (110 mg kg^{-1})	34.5 ± 0.42	1.5 ± 0.74	78.5 ± 0.76***	184.1 ± 0.60***
Group-V	MC-AgNPs (25 mg kg^{-1})	34.5 ± 0.42	1.66 ± 0.71	81.6 ± 0.88*	193.3 ± 0.88***
Group-VI	MC-AgNPs (50 mg kg^{-1})	34.5 ± 0.42	1.66 ± 0.71	93.5 ± 0.99***	210.6 ± 0.88***

3.8. Effect of treatments on motor coordination (rotarod test)

In the Rotarod test, diazepam-treated rats showed the shortest fall-off latency due to sedative effects. Both doses of HEMC improved motor performance, while MC-AgNPs produced a more pronounced improvement. The group that received the highest dose of MC-AgNPs had the longest fall-off latency (93.5 ± 0.99 s fall-off latency ($p < 0.0001$)), which means they had better neuromuscular coordination and less motor impairment. MC-AgNPs improved neuromuscular coordination: the MC extract (110 mg kg^{-1}) had an 81.33 ± 0.66 s fall-off latency, as shown (Fig. 9; Table 5).

Values are shown as mean ± SEM, $n = 6$, $p < 0.001$ *vs.* the control group, and ***$p < 0.001$ *versus* the normal group (one-way analysis of variance (ANOVA) followed by multiple comparisons). Multiple comparison test by Dunnett.

3.9. Effect of treatments on GABA in rat brain

The PTZ caused a significant reduction in brain GABA levels (1.93 ± 0.08 μmol g^{-1} tissue), supporting its known mechanism of inducing seizures through GABAergic inhibition. In contrast, diazepam effectively restored GABA levels to near-normal values (5.50 ± 0.07 μmol g^{-1} tissue). HEMC increased GABA levels in a dose-dependent manner (3.85 ± 0.07 and 4.10 ± 0.11 μmol g^{-1} tissue), while MC AgNPs produced a more pronounced effect. Notably, the high dose of MC AgNPs elevated GABA levels to 5.10 ± 0.14 μmol g^{-1} tissue, closely approaching those observed with diazepam ($p < 0.001$ *vs.* PTZ; $p > 0.05$ *vs.* diazepam) (Table 6, Fig. 10).

3.10. Effect of treatments on oxidative stress markers

SOD and GSH levels were significantly lower and MDA concentrations were significantly higher as a result of PTZ-induced significant oxidative stress. Diazepam restored antioxidant levels close to normal. HEMC exhibited moderate antioxidant activity, while MC-AgNPs produced a significant improvement across all biomarkers. High-dose MC-AgNPs markedly increased SOD and GSH (SOD (10.75 ± 0.19 U mg^{-1}), GSH (6.8 ± 0.08 μmol mg^{-1})), while reducing MDA levels (1.53 ± 0.12 nmol mg^{-1}), demonstrating strong antioxidant

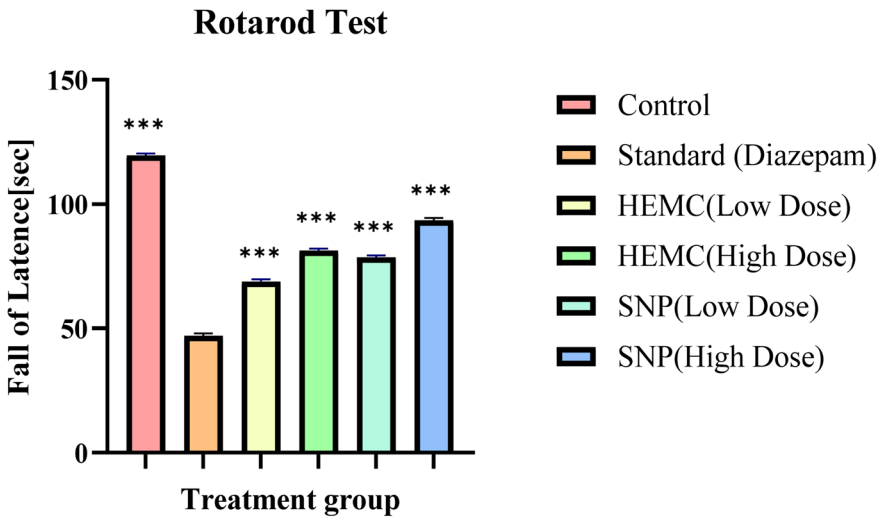

Fig. 9 Effect of treatment compounds of *Matricaria chamomilla* on fall-off latency of rats using rotarod test.

Table 5 Effect of treatments on motor coordination (Rotarod test)

Group	Treatment	Fall-off latency (sec, mean ± SEM, $n = 6$)
Group-I	Normal control	$119.8333 \pm 0.76^{***}$
Group-II	Standard (diazepam, 5 mg kg^{-1})	$47.16667 \pm 0.90^{***}$
Group-III	HEMC (55 mg kg^{-1})	$68.83 \pm 0.79^{***}$
Group-IV	HEMC (110 mg kg^{-1})	$81.33 \pm 0.66^{***}$
Group-V	MC-AgNPs (25 mg kg^{-1})	$78.5 \pm 0.76^{***}$
Group-VI	MC-AgNPs (50 mg kg^{-1})	$93.5 \pm 0.99^{***}$

potential and suggesting that oxidative stress attenuation contributes to its neuroprotective effect (Fig. 11; Table 7).

Values are shown as mean ± SEM, $n = 6$, $p < 0.001$ *vs.* the control group, and ***$p < 0.001$ *versus* the normal group (one-way analysis of variance (ANOVA) followed by multiple comparisons). Multiple comparison test by Dunnett.

3.11. Histopathological studies

The histopathological analysis of H&E-stained hippocampal sections (Fig. 12) was carried out, and neuronal damage was assessed using a blinded scoring system (0 = no damage, 1 = mild, 2 = moderate, 3 = severe) based on pyknosis, neuronal loss, and gliosis. Rats in the PTZ-treated group (group II) exhibited marked neuronal damage, including pronounced shrinkage, high levels of pyknosis (score 2.8 ± 0.2), and disrupted hippocampal architecture. In contrast, the diazepam-treated group (group III) largely preserved normal neuronal structure, showing only minimal pyknosis (score 0.3 ± 0.1). Treatment with HEMC provided partial neuroprotection in a dose-dependent manner, with moderate reductions in damage (group IV: 1.5 ± 0.2; group V: 1.2 ± 0.1). Notably, MC AgNPs demonstrated the most pronounced protective effect. The high-dose nanoparticle group (group VII) showed nearly normal hippocampal architecture with very low levels of pyknosis (score 0.5 ± 0.1), closely resembling the normal control group (group I: 0.0 ± 0.0). The comparative pyknosis scores in hippocampal sections (H&E stained, 40×) across experimental groups as shown in Fig. 12.

Table 6 Effect of treatments on neurotransmitter GABA in rat brain[a]

Group	Treatment	GABA (μg mg^{-1} protein, mean ± SEM)
Group-I	Normal control (vehicle)	5.50 ± 0.14
Group-II	PTZ-induced (80 mg kg^{-1})	1.93 ± 0.08
Group-III	Diazepam (5 mg kg^{-1}) + PTZ	$5.50 \pm 0.07^{***}$
Group-IV	HEMC (55 mg kg^{-1}) + PTZ	$3.85 \pm 0.07^{***}$
Group-V	HEMC (110 mg kg^{-1}) + PTZ	$4.10 \pm 0.11^{***}$
Group-VI	MC-AgNPs (25 mg kg^{-1}) + PTZ	$4.90 \pm 0.11^{***}$

[a] All data are mean ± SEM ($n = 6$). ***$p < 0.001$ *vs.* PTZ-induced group. One-way ANOVA followed by Tukey's post-hoc test.

4. Discussion

This study presents the first evidence that green-synthesized silver nanoparticles produced from *Matricaria chamomilla* (MC-AgNPs) have much greater anticonvulsant and neuroprotective effects than crude plant extract in a PTZ-induced epilepsy rat model. The findings support a green nanomedicine approach in which the plant extract is not just a source of bioactives, but also an active participant in nanofabrication, resulting in a synergistic therapeutic combination, hence increasing their therapeutic potential for central nervous system illnesses. The constant superiority of environmentally friendly synthesis MC-AgNPs in behavioral, biochemical, and histopathological endpoints demonstrates the successful conversion of green nanotechnology into a functioning neurotherapeutic.

4.1. Nanoparticle characteristics and their implications for efficacy

The effective synthesis of MC-AgNPs was validated by a prominent SPR peak at 420 nm, spherical morphology (SEM), and

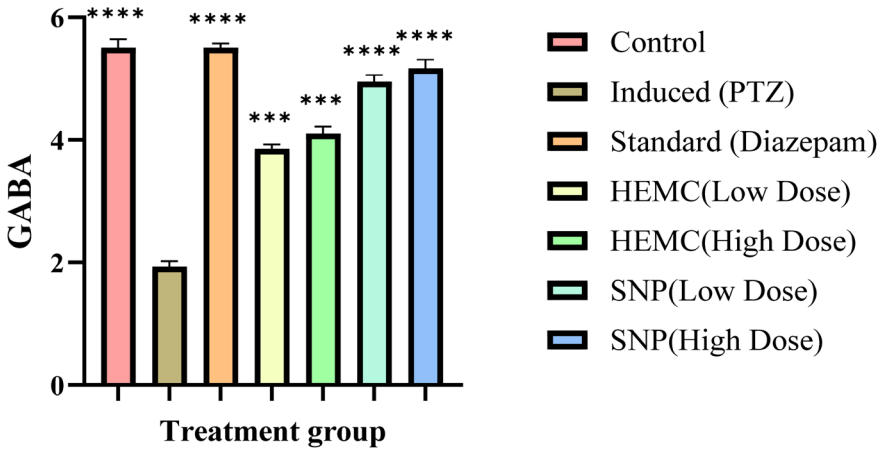

Fig. 10 Effect of treatment compounds of *Matricaria chamomilla* and its silver nanoparticle on GABA levels in rats brain.

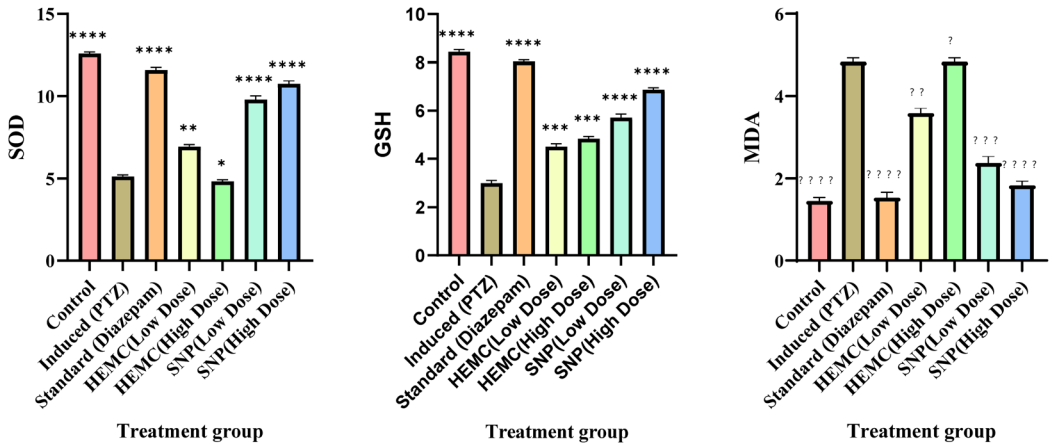

Fig. 11 Effect of treatment compounds of *Matricaria chamomilla* and its silver nanoparticle on superoxide dismutase, Glutathione and Malondialdehyde in rat's brain.

a moderate negative zeta potential (−8.9 ± 0.08 mV). The hydrodynamic diameter of ~274 nm and PDI of 0.312 suggest a moderately polydisperse population suitable for biological evaluation. The FTIR measurement showed the role of chamomile extract's phenolic and flavonoid groups in decreasing and capping the nanoparticles, resulting in a stable, biocompatible phytocomplex. This green synthesis strategy not only adheres to sustainable principles, but it also results in a synergistic entity in which the silver core and phytocapping agents may both contribute to the observed biological activity.[53,54] The negative surface charge, while indicating only limited colloidal stability, may have aided in reducing protein opsonization, thereby impacting *in vivo* distribution and brain exposure.[55]

Importantly, although chemically synthesized or uncoated silver nanoparticles have been linked to neurotoxic effects at higher doses, green-synthesized nanoparticles—especially

Table 7 Effect of treatments on oxidative stress markers[a]

Group	Treatment	SOD (U mg^{-1} protein, mean ± SEM)	GSH (μmol mg^{-1} protein, mean ± SEM)	MDA (nmol mg^{-1} protein, mean ± SEM)
Group-I	Normal control (vehicle)	12.50 ± 0.10	4.20 ± 0.09	1.45 ± 0.08
Group-II	PTZ-induced (80 mg kg^{-1})	5.10 ± 0.08	3.90 ± 0.11	4.80 ± 0.09
Group-III	Diazepam (5 mg kg^{-1}) + PTZ	11.60 ± 0.15 ***	8.30 ± 0.06 ***	1.53 ± 0.12 ***
Group-IV	HEMC (55 mg kg^{-1}) + PTZ	6.90 ± 0.12**	4.50 ± 0.13*	3.50 ± 0.12**
Group-V	HEMC (110 mg kg^{-1}) + PTZ	4.80 ± 0.09*	4.80 ± 0.09*	4.80 ± 0.09*
Group-VI	MC-AgNPs (25 mg kg^{-1}) + PTZ	9.80 ± 0.21 ***	5.71 ± 0.14 ***	2.36 ± 0.16 ***
Group-VII	MC-AgNPs (50 mg kg^{-1}) + PTZ	10.75 ± 0.19***	6.80 ± 0.08***	1.53 ± 0.11 ***

[a] Data are mean ± SEM ($n = 6$). *$p < 0.05$, **$p < 0.01$, ***$p < 0.001$ *vs.* PTZ-induced group. One-way ANOVA followed by Tukey's post-hoc test.

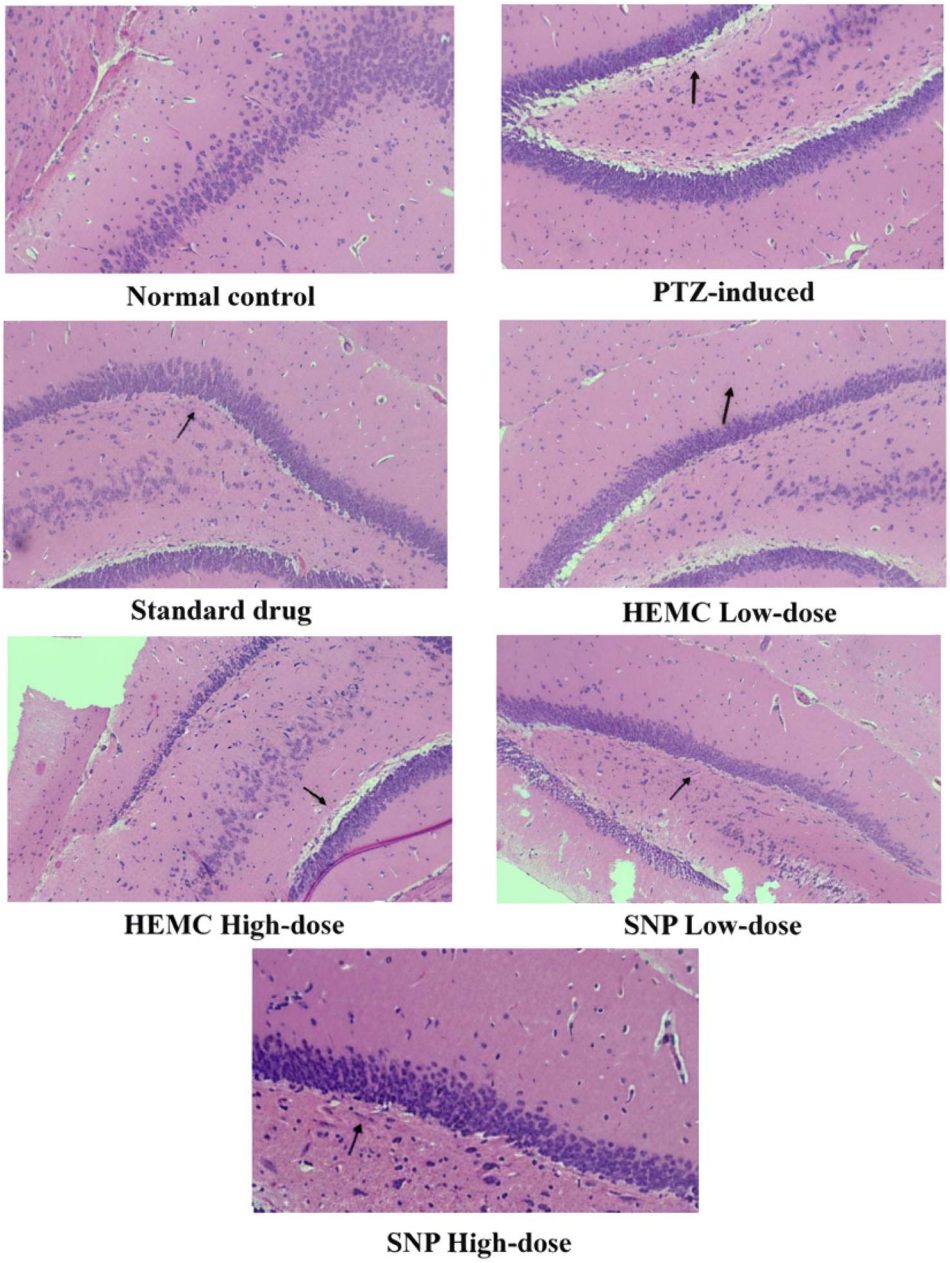

Fig. 12 Comparative pyknosis scores in hippocampal sections (H&E stained, 40×) across experimental groups. Group I (normal control) showed healthy neurons with clear nuclei and an absence of pyknosis. Group II (PTZ-induced) exhibited frequent pyknotic nuclei, neuronal shrinkage, and disrupted cytoarchitecture. Group III (standard drug) displayed preserved neuronal layers with rare or absent pyknosis. Group IV (low-dose MC extract) showed mostly intact neurons with occasional focal pyknosis, while group V (high-dose MC extract) exhibited well-preserved neurons with sparse pyknosis. Group VI (low-dose MCNP) displayed largely preserved neurons with occasional pyknosis, and group VII (high-dose MCNP) showed intact neuronal morphology with minimal or no pyknosis, closely resembling normal control.

those capped with phytochemicals like apigenin and quercetin—can instead show neuroprotective properties. The phytochemical coating not only helps stabilize the nanoparticles but also adds antioxidant and anti-inflammatory effects, which may help offset potential nanoparticle-induced toxicity. Previous studies have reported that plant-mediated AgNPs can reduce oxidative stress and improve cognitive function in neurological models.[28,45] Taken together, the cognitive improvements observed with the high dose of MC AgNPs are likely due to the combined, or synergistic, effects of the silver core and the bioactive phytochemical coating, rather than any inherent neurotoxic effect.

4.2. Mechanistic synergy: increased bioavailability and dual activity

Despite possessing identical phytoconstituents, MC-AgNPs demonstrated a significant improvement in seizure latency, severity, and mortality. The nanoscale size is most likely responsible for increasing the blood–brain barrier (BBB)

penetration of important flavonoids such as apigenin, a recognized positive allosteric modulator of GABA-A receptors.[56,57] Our neurochemical findings explicitly corroborate this: the high-dose MC-AgNP group restored brain GABA levels to near-normal levels, a result that was essentially identical to diazepam and greatly outperformed the extract. We propose that the nanoparticle serves as a protective carrier, sheltering labile flavonoids from degradation while facilitating their sustained release and tailored transport to neural regions.[58]

Beyond basic distribution, MC-AgNPs demonstrated a potent dual mechanism. First, they increased chamomile's naturally occurring GABAergic action. Second, they mounted a strong antioxidant defense, increasing SOD and GSH while decreasing lipid peroxidation (MDA)[59,60] The antioxidant impact was significantly stronger than that of the extract alone. While surface-bound flavonoids contribute to free radical scavenging, recent research reveals that biosynthetic AgNPs have inherent antioxidant and anti-inflammatory capabilities.[61] Thus, he therapeutic impact is likely the result of a synergistic interaction: the phytocapping compounds give specialized receptor-mediated activity (GABA regulation), whereas the nanometallic component contributes broad-spectrum redox homeostasis and may influence neuroinflammatory pathways.

4.3. Functional and structural correlates of neuroprotection

The functional benefits went beyond seizure control. MC-AgNPs successfully corrected PTZ-induced cognitive deficiencies in the passive avoidance test and improved motor coordination on the rotarod. These gains in learning, memory, and neuromuscular coordination are important indications of overall neuroprotection because they represent the integrity of the hippocampus and cerebellar circuits. The histological data provides the definitive structural correlate: treatment with high-dose MC-AgNPs resulted in hippocampus architecture with little pyknosis, which was similar to the normal control. This exceptional preservation of cytoarchitecture demonstrates the formulation's ability to prevent seizure-induced neuronal death, coupling biochemical repair (GABA, antioxidants) to tangible architectural salvage.

4.4. Positioning within nanomedicine and herbal drug development

This study combines the established discipline of ethnopharmacology with cutting-edge nanomedicine. While chamomile's neuroprotective qualities have been demonstrated in models of anxiety and neurotoxicity,[62,63] its use in epilepsy—particularly using a nano-delivery platform—is unique. Similarly, while plant-derived AgNPs are being studied for antibacterial and anticancer uses,[64–66] their utility in chronic neurological illnesses such as epilepsy is underexplored. Our study stands out by thoroughly illustrating how green nanoformulation can unlock and enhance the therapeutic potential of a common medicinal plant for a complicated neurological illness. It goes beyond basic proof-of-concept to present a multiparametric mechanistic explanation for the increased efficacy.[67]

4.5. Limits and future translational directions

While this study provides strong proof of concept, a few limitations should be considered. First, the low zeta potential (−8.9 mV) suggests limited electrostatic stabilization, which could increase the risk of nanoparticle aggregation in physiological fluids and potentially influence biodistribution and toxicity. However, the phytochemical capping layer likely provided steric stabilization, maintaining adequate colloidal integrity over the short dosing period, as reflected by the observed therapeutic effects. Second, although MC AgNPs showed better efficacy than the crude extract, suggesting improved bioavailability or brain penetration, this was not directly measured. Future pharmacokinetic studies are needed to compare brain levels of apigenin and other flavonoids following nanoformulation *versus* the crude extract. Third, while the 3-day pretreatment model demonstrates acute anticonvulsant effects, studies using chronic epilepsy models (*e.g.*, kindling) are needed to assess potential disease-modifying benefits fourth, EDX and XRD analyses were not carried out in this study. Including these techniques in future work would help confirm the elemental composition and crystallinity of the nanoparticles. Fifth, although high-dose MC AgNPs improved cognitive function here, the possibility of neurotoxicity—especially at higher doses or with prolonged use—cannot be overlooked. Long-term safety studies are needed, particularly to assess silver accumulation in the brain and other tissues. Finally, the exact molecular interactions at the nano–bio interface remain unclear. Further research should explore mechanisms such as effects on blood–brain barrier transporter expression and anti-inflammatory pathways, including NF-κB signaling and the NLRP3 inflammation. Additionally, this study did not include a comparison with standard chemically synthesized silver nanoparticles. Future work should incorporate such comparisons to better highlight the potential advantages of the green synthesis approach.

5. Conclusion

The present study shows that green-synthesized Matricaria chamomilla silver nanoparticles (MC AgNPs) have strong anticonvulsant and neuroprotective effects in a PTZ-induced acute seizure model in rats. Treatment with MC AgNPs delayed the onset of seizures, reduced their frequency and severity, and improved both cognitive and motor functions. In addition, they helped restore brain GABA levels and brought oxidative stress markers closer to normal. Histopathological findings further supported these results, showing clear preservation of neuronal structure, particularly in the hippocampus. Notably, MC AgNPs consistently performed better than the crude ethanolic extract, indicating that the nanoformulation enhances the therapeutic potential of chamomile's bioactive compounds. This improvement is likely due to better bioavailability and a combined effect on GABAergic signaling and antioxidant defenses. Overall, these findings suggest that MC AgNPs could serve as a promising, cost-effective, plant-based adjunct approach for epilepsy management. However, further studies are needed to evaluate

their effects in chronic epilepsy models, understand their pharmacokinetics, assess long-term safety, and clarify the exact molecular mechanisms responsible for their neuroprotective action.

Ethical statement

The study was approved by the Institutional Animal Ethics Committee of Al-Ameen College of Pharmacy, Bengaluru, Karnataka, the approval No. (AACP/IAEC/41/MARCH 2025/09), (a total of 42 winster albino rats) and conducted in accordance with CPCSEA guidelines. All the animals receive human care according to the criteria outlined in the "Guide for the Care and Use of Laboratory Animals" prepared by the "National Academy of Sciences" and published by the "National Institute of Health" which is based on the principles of the Declaration of Helsinki. We followed the ARRIVE guidelines (https://arriveguidelines.org).

Author contributions

Conceptualization, R.K.M., Y.A., and M.R.; methodology, K.K., Y.A. and M.C.; software, Y.A. and M.M.A.; validation, S.A.F., and I.P.; formal analysis, R.K.M. and M.C.; investigation, M.C. and K.K.; resources, H.A. and S.A.F.; data curation, T.B.S., Y.A., and H.A.; writing—original draft preparation, R.K.M. and K.K.; writing-review and editing, M.R., M.M.A. and Y.A,; visualization, I.P., T.B.S. and M.R.; supervision, M.R., and R.K.M.; project administration, R.K.M.; funding acquisition, M.R.

Conflicts of interest

The authors declare no conflicts of interest.

Data availability

All data analyzed or generated during this study are included in this article and supplementary information (SI). Supplementary information: Fig. S1: standard curve for Gallic acid, Fig. S2: standard curve for quercetin, Fig. S3: UV-visible graph of *Matricaria chamomilla* ethanolic extract. See DOI: https://doi.org/10.1039/d6ra01236a.

Acknowledgements

The authors extend their appreciation to the Deanship of Research and Graduate Studies at King Khalid University for funding this work through the Large research Project under grant number RGP2/233/46. The author would like to thank the Deanship of Scientific Research at Shaqra University for supporting this work.

References

1 R. S. Fisher, W. van Emde Boas, W. Blume, *et al.*, Epileptic seizures and epilepsy: definitions proposed by the International League Against Epilepsy (ILAE) and the International Bureau for Epilepsy (IBE), *Epilepsia*, 2005, **46**(4), 470–472.
2 World Health Organization, *Epilepsy*, Geneva, WHO, 2022.
3 S. Wang, H. Zhang, R. Li, Z. Liu and D. Xiang, Altered Neuroplasticity in Epilepsy is Associated with Neuroinflammation and Oxidative Stress: In vivo Evidence of Brain-Derived Extracellular Vesicles, *Int. J. Nanomed.*, 2025, **20**, 7185–7197, DOI: 10.2147/IJN.S514559.
4 I. E. Scheffer, S. Berkovic, G. Capovilla, *et al.*, ILAE classification of the epilepsies: position paper of the ILAE Commission for Classification and Terminology, *Epilepsia*, 2017, **58**(4), 512–521.
5 R. S. Fisher, C. Acevedo, A. Arzimanoglou, *et al.*, ILAE official report: A practical clinical definition of epilepsy, *Epilepsia*, 2014, **55**(4), 475–482.
6 D. J. Thurman, E. Beghi, C. E. Begley, *et al.*, Standards for epidemiologic studies and surveillance of epilepsy, *Epilepsia*, 2011, **52**(Suppl 7), 2–26.
7 P. Kwan, A. Arzimanoglou, A. T. Berg, *et al.*, Definition of drug resistant epilepsy: consensus proposal by the ad hoc Task Force of the ILAE Commission on Therapeutic Strategies, *Epilepsia*, 2010, **51**(6), 1069–1077.
8 A. K. Ngugi, C. Bottomley, I. Kleinschmidt, J. W. Sander and C. R. Newton, Estimation of the burden of active and lifetime epilepsy: a meta-analytic approach, *Epilepsia*, 2010, **51**(5), 883–890.
9 K. M. Fiest, K. M. Sauro, S. Wiebe, *et al.*, Prevalence and incidence of epilepsy: a systematic review and meta-analysis of international studies, *Neurology*, 2017, **88**(3), 296–303.
10 C. R. Newton and H. H. Garcia, Epilepsy in poor regions of the world, *Lancet*, 2012, **380**, 1193–1201.
11 Á. B. Monteiro, A. F. Alves, A. C. Ribeiro Portela, H. F. Oliveira Pires, M. Pessoa de Melo, N. M. Medeiros Vilar Barbosa and C. F. Bezerra Felipe, Pentylenetetrazole: A review, *Neurochem. Int.*, 2024, **180**, 105841, DOI: 10.1016/j.neuint.2024.105841.
12 M. Hashemian, M. Ghasemi-Kasman, S. Ghasemi, A. Akbari, M. Moalem-Banhangi, L. Zare and S. R. Ahmadian, Fabrication and evaluation of novel quercetin-conjugated Fe3O4–β-cyclodextrin nanoparticles for potential use in epilepsy disorder, *Int. J. Nanomed.*, 2019, **14**, 6481–6495, DOI: 10.2147/IJN.S218317.
13 A. A. Alshehri and M. A. Malik, Phytomediated Photo-Induced Green Synthesis of Silver Nanoparticles Using Matricaria chamomilla L. and Its Catalytic Activity against Rhodamine B, *Biomolecules*, 2020, **10**(12), 1604.
14 M. Dadashpour, A. Firouzi-Amandi, M. Pourhassan-Moghaddam, *et al.*, Biomimetic synthesis of silver nanoparticles using *Matricaria chamomilla* extract and their potential anticancer activity against human lung cancer cells, *Mater. Sci. Eng., C*, 2018, **92**, 902–912.
15 M. A. El, J. C. G. Esteves da Silva, S. Charfi, M. E. Candela Castillo, A. Lamarti and M. B. Arnao, Chamomile (*Matricaria chamomilla* L.): A Review of Ethnomedicinal Use, Phytochemistry and Pharmacological Uses, *Life*, 2022, **12**(4), 479.

16 A. N. Jikah and G. I. Edo, Moringa oleifera: a valuable insight into recent advances in medicinal uses and pharmacological activities, *J. Sci. Food Agric.*, 2023, **103**(15), 7343–7361, DOI: 10.1002/jsfa.12892.
17 A. Kazemi, S. Shojaei-Zarghani, P. Eskandarzadeh and M. H. Hashempur, Effects of chamomile (*Matricaria chamomilla* L.) on sleep: A systematic review and meta-analysis of clinical trials, *BMC Complementary Med. Ther.*, 2024, **84**, 103071, DOI: 10.1016/j.ctim.2024.103071.
18 G. U. Khan, S. S. Khan, S. Naeem, *et al.*, *Matricaria chamomilla* L. leaf and flower extracts improved scopolamine-induced amnesia via regulation of cholinergic dysfunction and brain antioxidant status: An in-vivo and in-silico study, *J. Ethnopharmacol.*, 2025, **352**, 120141, DOI: 10.1016/j.jep.2025.120141.
19 F. Mohsenzadeh-Ledari, M. Agajani Delavar, A. A. Moghadamnia, *et al.*, Efficacy and safety of *Matricaria chamomilla* intervention in managing menopausal symptoms: a triple-blind clinical trial, *Menopause*, 2025, **32**(4), 353–358, DOI: 10.1097/GME.0000000000002496.
20 Y.-L. Dai, Y. Li, Q. Wang, F.-J. Niu, K.-W. Li, Y.-Y. Wang, J. Wang, C.-Z. Zhou and L.-N. Gao, Chamomile: A Review of Its Traditional Uses, Chemical Constituents, Pharmacological Activities and Quality Control Studies, *Molecules*, 2023, **28**(1), 133, DOI: 10.3390/molecules28010133.
21 J.-L. Ríos, G. R. Schinella and I. Moragrega, Phenolics as GABAA Receptor Ligands: An Updated Review, *Molecules*, 2022, **27**(6), 1770, DOI: 10.3390/molecules27061770.
22 R. Della Loggia, R. Carle, S. Sosa and A. Tubaro, Evaluation of the anti-inflammatory activity of chamomile preparations, *Planta Med.*, 1990, **56**(6), 657–658.
23 M. Spinella, Herbal medicines and epilepsy: the potential for benefit and adverse effects, *Epilepsy Behav.*, 2001, **2**(6), 524–532.
24 J. Cai, H. Yang, Z. He and C. Wu, Intelligent Nanomedicine Systems Utilizing Diverse Nanoparticles for Osteosarcoma Therapy: A Review, *Int. J. Nanomed.*, 2025, **20**, 14115–14130, DOI: 10.2147/IJN.S560865.
25 D. B. Mejjo, R. Nayal, W. Abdelwahed and M. Y. Abajy, Anti-Arthritis and Biosafety Properties of Green Synthesized Zinc Oxide Nanoparticles Loaded with Cedrus libani Extract, *Int. J. Nanomed.*, 2025, **20**, 11525–11551, DOI: 10.2147/IJN.S537934.
26 M. Murshed, J. Al-Tamimi, M. M. Mares, W. A. Q. Hailan, K. E. Ibrahim and S. Al-Quraishy, Pharmacological Effects of Biosynthesis Silver Nanoparticles Utilizing Calotropis procera Leaf Extracts on Plasmodium berghei-Infected Liver in Experiment Mice, *Int. J. Nanomed.*, 2024, **19**, 13717–13733, DOI: 10.2147/IJN.S490119.
27 S. S. Alghamdi, H. A. Alhaidal, A. E. Mohammed, A. Alsubait, M. D. Alshammari, L. Alsaqer, S. S. Alzahrani, *et al.*, A Novel Integrated Approach: Plant-Mediated Synthesis, in Vitro and in Silico Evaluation of Silver Nanoparticles for Breast Cancer and Bacterial Therapies, *Int. J. Nanomed.*, 2025, 10043–10071, DOI: 10.2147/IJN.S516723.
28 A. Sharma, J. V. Sanjay, M. Park and H. J. Lee, Biogenic silver NPs alleviate LPS-induced neuroinflammation in a human fetal brain-derived cell line: Molecular switch to the M2 phenotype, modulation of TLR4/MyD88 and Nrf2/HO-1 signaling pathways, and molecular docking analysis, *Biomater. Adv.*, 2023, **148**, 213363, DOI: 10.1016/j.bioadv.2023.213363.
29 S. Suleiman and J. Hassan, The effects of crude alkaloid extract of *Matricaria chamomilla* L. on convulsions induced by pentylenetetrazole in chicks, *J. Vet. Res.*, 2022, **21**(3), 31–41.
30 D. O. Kim, S. W. Jeong and C. Y. Lee, Antioxidant capacity of phenolic phytochemicals from various cultivars of plums, *Food Chem.*, 2003, **81**(3), 321–326.
31 N. Saeed, M. R. Khan and M. Shabbir, Antioxidant activity, total phenolic and total flavonoid contents of whole plant extracts of Torilis leptophylla L, *BMC Complementary Altern. Med.*, 2012, **12**, 221.
32 C. C. Chang, M. H. Yang, H. M. Wen and J. C. Chern, Estimation of total flavonoid content in propolis by two complementary colorimetric methods, *J. Food Drug Anal.*, 2002, **10**(3), 178–182.
33 T. Rajeshwari, R. Suresh and M. Sudhakar, Phytochemical investigation and antioxidant potential of two Amaranthaceae plants: Achyranthes aspera Linn and Chenopodium album Linn, *Int. J. Res. Pharm. Sci.*, 2022, **13**(2), 902–911.
34 D. J. Beale, F. R. Pinu, K. A. Kouremenos, *et al.*, Review of recent developments in GC–MS approaches to metabolomics-based research, *Metabolomics*, 2018, **14**, 152.
35 A. Elias, P. V. Habbu and S. Iliger, Preparation, characterization and screening of silver nanoparticles using phenolic rich fractions of Amaranthus gangeticus L. for its in-vitro antioxidant, anti-diabetic and anti-cancer activities, *RGUHS J. Pharm. Sci.*, 2021, **11**(3), DOI: 10.26463/rjps.11_3_5.
36 R. Díaz-Puertas, F. J. Álvarez-Martínez, E. Rodríguez-Cañas, *et al.*, An Innovative Approach Based on the Green Synthesis of Silver Nanoparticles Using Pomegranate Peel Extract for Antibacterial Purposes, *Bioinorg. Chem. Appl.*, 2025, **2025**, 2009069, DOI: 10.1155/bca/2009069.
37 P. Singh and I. Mijakovic, Strain-Specific Bacillus subtilis-Derived Silver Nanoparticles for Effective Antibacterial Activity Against Multidrug-Resistant Pathogens: In Vitro Model, *Int. J. Nanomed.*, 2025, **20**, 13055–13078, DOI: 10.2147/IJN.S527950.
38 E. Rauch, C. Ari, D. P. D'Agostino and Z. Kovács, Exogenous Ketone Supplementation Enhances the Anti-Epileptic Effect of Levetiracetam in Wistar Albino Glaxo/Rijswijk Rats, *Nutrients*, 2025, **17**(10), 1721, DOI: 10.3390/nu17101721.
39 G. L. Viswanatha, M. V. Venkataranganna, N. B. Prasad and G. Ashok, Evaluation of anti-epileptic activity of leaf extracts of Punica granatum on experimental models of epilepsy in mice, *J. Intercult. Ethnopharmacol.*, 2016, **5**(4), 415–420.
40 A. Showraki, M. Emamghoreishi and S. Oftadegan, Anticonvulsant effect of the aqueous extract and essential

oil of Carum carvi L. seeds in a pentylenetetrazole model of seizure in mice, *Iran. J. Med. Sci.*, 2016, **41**(3), 200–207.

41 A. Tourov, *et al.*, Spike morphology in PTZ-induced generalized and cobalt-induced partial experimental epilepsy, *Funct. Neurol.*, 1996, **11**(5), 237–245.

42 H. M. Gamal El-Deen, A. E. Essawy, N. A. Mohammed, M. S. Abdelfattah, A. S. Fathalla, M. F. El-Khadragy and A. E. Abdel Moniem, Epigallocatechin-3-gallate conjugated with selenium nanoparticles prevents neurological complications in rats exhibiting schizophrenia-like behaviors, *Front. Pharmacol*, 2025, **16**, 1680380, DOI: 10.3389/fphar.2025.1680380.

43 A. Lüttjohann, P. F. Fabene and G. van Luijtelaar, A revised Racine's scale for PTZ-induced seizures in rats, *Physiol. Behav.*, 2009, **98**(5), 579–586, DOI: 10.1016/j.physbeh.2009.09.005.

44 R. J. Racine, Modification of seizure activity by electrical stimulation. II. Motor seizure, *Electroencephalogr. Clin. Neurophysiol.*, 1972, **32**(3), 281–294, DOI: 10.1016/0013-4694(72)90177-0.

45 X. Yuan, Z. Fu, P. Ji, L. Guo, A. O. Al-Ghamdy, A. Alkandiri, O. A. Habotta, A. E. Abdel Moneim and R. B. Kassab, Selenium Nanoparticles Pre-Treatment Reverse Behavioral, Oxidative Damage, Neuronal Loss and Neurochemical Alterations in Pentylenetetrazole-Induced Epileptic Seizures in Mice, *Int. J. Nanomed.*, 2020, **15**, 6339–6353, DOI: 10.2147/IJN.S259134.

46 B. Afzalipour, M. Khaksari, N. Nakhaee and M. Shabani, Neuroprotective effects of ellagic acid on cognitive deficits induced by PTZ in male rats: involvement of oxidative stress and mitochondrial function, *Epilepsy Behav.*, 2019, **92**, 290–296.

47 Q. Zheng, S. L. Xu, X. L. Guo, C. Y. Wang, M. D. Ma and J. F. Ge, Effects of melatonin on the pharmacokinetics and amino acid metabolism profile of vigabatrin in rats, *Toxicol. Appl. Pharmacol.*, 2025, **496**, 117247, DOI: 10.1016/j.taap.2025.117247.

48 E. Khalilzadeh, A. Ahmadiani and R. Ghasemi, Enriched environment improves cognitive dysfunction in PTZ-treated rats through inhibition of oxidative stress and apoptosis, *Epilepsy Behav.*, 2020, **102**, 106651.

49 M. Rahmati, M. Khalili and M. Roghani, The effects of vitexin on motor coordination and memory impairment induced by pentylenetetrazole in rats, *Avicenna J. Phytomed.*, 2019, **9**(2), 129–139.

50 Z. Sayyar, A. Yazdinezhad, M. Hassan and I. Jafari Anarkooli, Protective Effect of *Matricaria chamomilla* Ethanolic Extract on Hippocampal Neuron Damage in Rats Exposed to Formaldehyde, *Oxid. Med. Cell. Longev.*, 2018, **2018**, 6414317, DOI: 10.1155/2018/6414317.

51 M. Górny, P. Górnaś, A. Górska, *et al.*, Alterations in antioxidant enzyme activities in the neurodevelopmental rat model of schizophrenia induced by glutathione deficiency, *Front. Neurosci.*, 2015, **9**, 299.

52 T. H. Kim, J. Choi, H. G. Kim and H. R. Kim, Quantification of neurotransmitters in mouse brain tissue by using liquid chromatography coupled electrospray tandem mass spectrometry, *J. Anal. Methods Chem.*, 2014, **2014**, 506870, DOI: 10.1155/2014/506870.

53 B. H. Kiani, I. Arshad, S. Najeeb, *et al.*, Evaluation of Biogenic Silver Nanoparticles Synthesized from Vegetable Waste, *Int. J. Nanomed.*, 2023, **18**, 6527–6544, DOI: 10.2147/IJN.S432252.

54 S. Bawazeer, Green Synthesis: An Eco-Friendly Approach for the Synthesis of Silver Nanoparticles Functionalized with Operculina turpethum and It's In vitro and in vivo Biological Activities, *Int. J. Nanomed.*, 2025, **20**, 2991–3005, DOI: 10.2147/IJN.S507134.

55 E. Fröhlich, The role of surface charge in cellular uptake and cytotoxicity of medical nanoparticles, *Int. J. Nanomed.*, 2012, **7**, 5577–5591, DOI: 10.2147/IJN.S36111.

56 C. Saraiva, C. Praça, R. Ferreira, T. Santos, L. Ferreira and L. Bernardino, Nanoparticle-mediated brain drug delivery: Overcoming blood–brain barrier to treat neurodegenerative diseases, *J. Contr. Release*, 2016, **235**, 34–47, DOI: 10.1016/j.jconrel.2016.05.044.

57 R. Avallone, P. Zanoli, G. Puia, M. Kleinschnitz, P. Schreier and M. Baraldi, Pharmacological profile of apigenin, a flavonoid isolated from *Matricaria chamomilla*, *Biochem. Pharmacol.*, 2000, **59**(11), 1387–1394, DOI: 10.1016/s0006-2952(00)00264-1.

58 J. K. Patra, G. Das, L. F. Fraceto, *et al.*, Nano based drug delivery systems: recent developments and future prospects, *J. Nanobiotechnol.*, 2018, **16**(1), 71, DOI: 10.1186/s12951-018-0392-8.

59 C. M. Cremer, N. Palomero-Gallagher, H. J. Bidmon, A. Schleicher, E. J. Speckmann and K. Zilles, Pentylenetetrazole-induced seizures affect binding site densities for GABA, glutamate and adenosine receptors in the rat brain, *Neuroscience*, 2009, **163**(1), 490–499, DOI: 10.1016/j.neuroscience.2009.03.068.

60 G. Das, H. S. Shin, I. J. Yang, L. T. H. Nguyen and J. K. Patra, Silk Biowaste Protein Mediated Silver Nanoparticles Synthesis and Analysis of Anti-Inflammatory, Wound Healing, Antidiabetic, Antioxidant, Tyrosinase Inhibition, and Antibacterial Mechanism of Action, *Int. J. Nanomed.*, 2025, **20**, 6551–6571, DOI: 10.2147/IJN.S512524.

61 A. Karnwal, A. Y. Jassim, A. A. Mohammed, V. Sharma, A. R. M. S. Al-Tawaha and I. Sivanesan, Nanotechnology for Healthcare: Plant-Derived Nanoparticles in Disease Treatment and Regenerative Medicine, *Pharmaceuticals*, 2024, **17**(12), 1711, DOI: 10.3390/ph17121711.

62 J. K. Srivastava, E. Shankar and S. Gupta, Chamomile: A herbal medicine of the past with bright future, *Mol. Med. Rep.*, 2010, **3**(6), 895–901, DOI: 10.3892/mmr.2010.377.

63 F. Alipour, F. Valizadegan, B. Seyedalipour and H. Babanezhad, Effect of *Matricaria chamomilla* flower extract on ethanol-induced hippocampal oxidative stress and behavioral disorder of anxiety and memory based on test-retest paradigm, *Int. J. Environ. Health Res.*, 2025, 1–11., DOI: 10.1080/09603123.2025.2579083.

64 C. Keskin, S. Aslan, M. F. Baran, *et al.*, Green Synthesis and Characterization of Silver Nanoparticles Using Anchusa Officinalis: Antimicrobial and Cytotoxic Potential, *Int. J. Nanomed.*, 2025, **20**, 4481–4502, DOI: 10.2147/IJN.S511217.

65 S. Devanesan, K. Ponmurugan, M. S. AlSalhi and N. A. Al-Dhabi, Cytotoxic and Antimicrobial Efficacy of Silver Nanoparticles Synthesized Using a Traditional Phytoproduct, Asafoetida Gum, *Int. J. Nanomed.*, 2020, **15**, 4351–4362, DOI: 10.2147/IJN.S258319.

66 J. Joseph, K. Z. Khor, E. J. Moses, V. Lim, M. Y. Aziz and N. Abdul Samad, In vitro Anticancer Effects of Vernonia amygdalina Leaf Extract and Green-Synthesised Silver Nanoparticles, *Int. J. Nanomed.*, 2021, **16**, 3599–3612, DOI: 10.2147/IJN.S303921.

67 X. Zhao, Z. Xu, D. Wang, *et al.*, Nanotechnology-based targeted regulation of NLRP3 Inflammasome: therapeutic strategies and clinical application prospects in inflammatory diseases, *Drug Deliv.*, 2025, **32**(1), 2580730, DOI: 10.1080/10717544.2025.2580730.